

Manifestation of Spin Correlations in Monocrystalline $\text{ErAl}_3(\text{BO}_3)_4$

Cite as: Low Temp. Phys. **45**, 1041 (2019); <https://doi.org/10.1063/1.5121279>
Published Online: 27 September 2019

V. A. Bedarev, D. N. Merenkov, M. I. Kobets, et al.



View Online



Export Citation



CrossMark

ARTICLES YOU MAY BE INTERESTED IN

[Magnetic and structural correlations in the warwickite \$\text{Mn}_2\text{OBO}_3\$](#)

Low Temperature Physics **45**, 1046 (2019); <https://doi.org/10.1063/1.5121280>

[Features of electronic paramagnetic resonance in the \$\text{ErAl}_3\(\text{BO}_3\)_4\$ single crystal](#)

Low Temperature Physics **44**, 863 (2018); <https://doi.org/10.1063/1.5049175>

[Coulomb effects on thermally induced shuttling of spin-polarized electrons](#)

Low Temperature Physics **45**, 1032 (2019); <https://doi.org/10.1063/1.5121274>

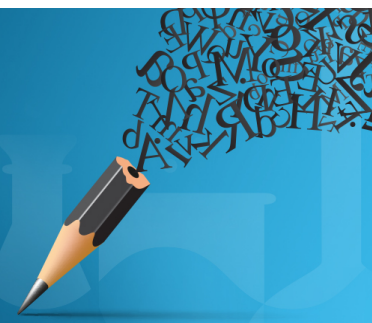


Author Services

English Language Editing

High-quality assistance from subject specialists

LEARN MORE



Manifestation of Spin Correlations in Monocrystalline $\text{ErAl}_3(\text{BO}_3)_4$

Cite as: Fiz. Nizk. Temp. **45**, 1217-1222 (September 2019); doi: 10.1063/1.5121279

Submitted: 23 July 2019



View Online



Export Citation



CrossMark

V. A. Bedarev,^{1,a)} D. N. Merenkov,¹ M. I. Kobets,¹ A. A. Zvyagin,¹ S. N. Poperezhai,¹ S. L. Gnatchenko,¹ T. Zajarniuk,² T. Vasevych,² M. U. Gutowska,² A. Szweczyk,² and I. A. Gudim³

AFFILIATIONS

¹B.Verkin Institute for Low Temperature Physics and Engineering of the National Academy of Sciences of Ukraine, 47 Nauky Ave., Kharkiv, 61103, Ukraine

²Institute of Physics, Polish Academy of Sciences, Warsaw, Poland

³L.V. Kirensky Institute of Physics, Federal Research Center KSC Siberian Branch of the Russian Academy of Sciences, Krasnoyarsk 660036, Russia

^{a)}Email: bedarev@ilt.kharkov.ua

ABSTRACT

A substantial magnetic contribution into specific heat capacity is found in monocrystalline $\text{ErAl}_3(\text{BO}_3)_4$ at temperatures below 5 K. The results of measured ESR spectra at 4,2 K confirm manifestation of short-range magnetic order as well. The obtained data is discussed invoking the model accounting for spin-spin interaction between rare-earth ions in paired clusters.

Published under license by AIP Publishing. <https://doi.org/10.1063/1.5121279>

1. INTRODUCTION

Rare-earth aluminum borates $\text{RAl}_3(\text{BO}_3)_4$ (R stands for a rare-earth element) possess trigonal space group with no inversion center and reveal pronounced nonlinear¹ and luminescent² optical properties. In these crystals, the giant magnetoelectric effect has been recently discovered.³ It has been shown that rare-earth aluminum borates can be promising materials for magnetic cooling.⁴

An interesting compound from this family is crystalline $\text{ErAl}_3(\text{BO}_3)_4$, which demonstrates a large magnetoelectric effect and highly anisotropic magnetic properties.⁵ Magnetometry of erbium aluminum borate has been carried out⁵ along with optical and magneto-optical spectroscopy and luminescence.^{6,7}

An additional line in electron spin resonance (ESR) spectrum of $\text{ErAl}_3(\text{BO}_3)_4$ at temperature 4,2 K has been reported in work.⁸ It has been supposed that this line appears due to the presence of magnetic clusters as a result of the substitution of Al^{3+} by Er^{3+} ions in the crystal. However, the phase transition to a magneto-ordered state in $\text{ErAl}_3(\text{BO}_3)_4$ has not been yet discovered, and it has been reported that the crystal is still paramagnetic at 2 K,⁵ implying another reason of the formation of magnetic clusters — the emergence of the phase transition. At least one of the rare-earth aluminum borate family — crystalline $\text{TbAl}_3(\text{BO}_3)_4$ — demonstrates a transition to magneto-ordered state (at $T = 0,68$ K).⁹ Therefore, it is worth to consider the possibility of manifestation of the short-range

order, which originates from spin-spin interaction between Er^{3+} ions in the crystalline lattice already at the temperature of liquid helium.

Our previous investigation of ESR spectra⁸ was supplemented with new data to resolve the question of spin correlations in $\text{ErAl}_3(\text{BO}_3)_4$. Moreover, since results of calorimetric studies can offer valuable information about the magnetic state of the crystal, we also measured specific heat capacity in a sufficiently wide temperature range.

2. EXPERIMENTAL

An additional investigation of the ESR spectrum of monocrystalline $\text{ErAl}_3(\text{BO}_3)_4$ was conducted at $T = 4,2$ K in external field \mathbf{H} applied in the plane ac , where a -axis is a second-order crystallographic axis, and the direction of c -axis coincides with the trigonal axis of the crystal. The conditions of an additional experiment were identical to the ones in work.⁸ In agreements with the previous results, at $\nu = 29,87$ GHz and $\mathbf{H} \parallel c$, the ESR spectrum demonstrated an additional low-intensity line in small fields [Fig. 1(a)] and an intensive line in a wide interval of bigger fields — approximately from 6 to 18 kOe [Fig. 1(b)]. At a certain deviation of \mathbf{H} from the direction of the c -axis in the mentioned range of magnetic field, three narrower lines of different intensity were observed instead of one wide line. This experimental fact is illustrated in Fig. 1(c) and (d). It can be observed that the intensity

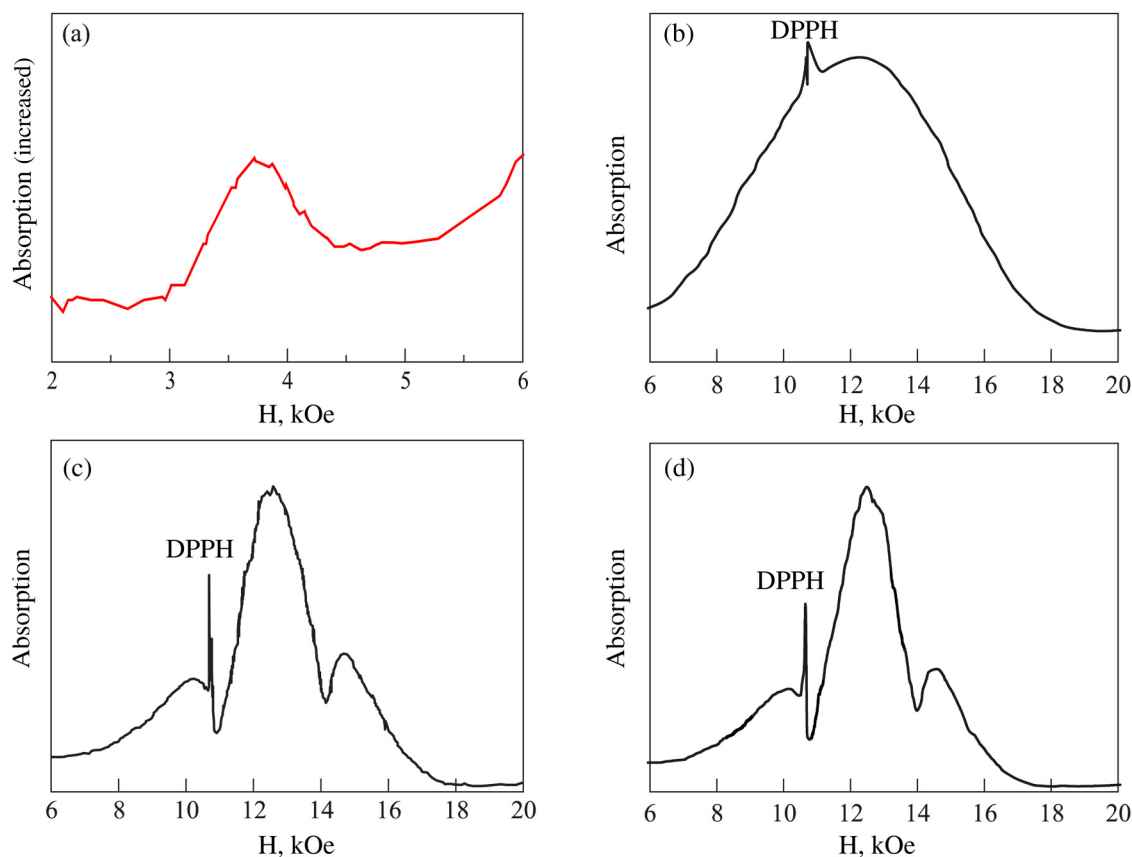


FIG. 1. ESR absorption spectra of monocrystalline $\text{ErAl}_3(\text{BO}_3)_4$ measured at $T = 4.2$ K at frequency $\nu = 29.87$ GHz (a), (b) — external field $\mathbf{H} \parallel c$, (c) \mathbf{H} is inclined in the ac plane at 2° from c -axis, (d) — at 5° from c -axis. To conveniently compare the results, intensity of the additional line (a) is magnified against intensity of the main line (b)–(d). The narrow lines (b)–(d) correspond to a signal from etalon sample of diphenylpicrylhydrazyl (DPPH).

maxima of sidelines are situated below the maximum of the central line and distant from it at approximately 2,2 kOe each.

Apparently, when \mathbf{H} is oriented strictly along the c -axis, the central and sidelines merge and become unresolvable, and at a slight deviation of field, it is possible to separate them due to the angle dependence of their intensities. At a further increasing deviation of \mathbf{H} from the c -axis, intensities of the sidelines decrease against the central line, and at angles larger than 8° , the sidelines are not observable.

Hence, transformation of the intense line into the triplet structure in the ESR spectra of monocrystalline $\text{ErAl}_3(\text{BO}_3)_4$ was revealed in parallel with a weak additional line. The experimental data is not explainable, accepting the existence of only isolated centers of absorption in the crystal. Broadly, the results of ESR studies indicated the occurrence of the short-range order in erbium aluminum borate. Such an order can appear due to the formation of magnetically ordered groups consisting of several erbium ions (pairs, triples, etc.) designated as magnetic clusters. It is known that the resonance on magnetic clusters has been observed earlier^{10,11} in the case of quasi-one-dimensional magnetic crystals.

According to the model,¹⁰ thermal excitation will cause some ions in clusters to have magnetic moments opposite to magnetic moments of the ground state and to the direction of the external field \mathbf{H} . One or several of the ground state ions in the vicinity of the thermally excited ones can, in turn, be already excited with microwave irradiating the crystal that changes the direction of their magnetic moments to the opposite and thus, enlarges the size of the excited group. As a consequence of such flips, one can observe spin-cluster resonance.

We can suppose that a similar situation occurs also in erbium aluminum borate. In this case, appearance of the additional low-intensity line [Fig. 1(a)] occurs due to the flip of a pair of moments upon absorption of one quantum of microwave field, and the triplet structure replaces the main line [Figs. 1(c) and 1(d)], which arises due to the flip of one magnetic moment in a cluster. One could expect that the triplet structure in the ESR spectrum will manifest itself at the magnetic field applied along the a -axis or with a slight deviation from the a -axis. In this case, the triplet structure was not observed yet. Possibly, the sidelines here are much less shifted from the central line than in Figs. 1(c) and 1(d), making it difficult to resolve the triplet structure.

From the model developed in work,¹⁰ the g -factor of an additional line g_2 must be twice as high as the g -factor of the intensive line g_1 , and the initial splitting of the additional line Δ_2 must be by two times larger than the splitting of the triplet sideline Δ_1 . As we established earlier,⁸ at $\mathbf{H} \parallel a$ the magnitude of the g -factor of the additional line $g_{2a} \approx 19,5$, and for the intensive line $g_{1a} \approx 9,5$. At $\mathbf{H} \parallel c$, the values of the g -factors are $g_{2c} \approx 3,4$ and $g_{1c} \approx 1,6$, respectively. Therefore, the ratio of g -factors ≈ 2 in both cases. We defined the initial splitting of the additional line as $\Delta_{2a} \approx 20$ GHz (0,96 K) and $\Delta_{2c} \approx 7$ GHz (0,33 K). A rough estimate of the initial splitting of the sideline inferred from spectral measurements, which are shown in Fig. 1(c), gives $\Delta_{1c} \approx 4,5$ GHz. Probably, the specified parameters should be defined more accurately. Nevertheless, we note a fairly good agreement of the experimental data and the spin-cluster resonance model.¹⁰

The fine structure of the ESR line of magneto-concentrated $\text{ErAl}_3(\text{BO}_3)_4$ can be described via spin-spin interactions of the absorbing Er^{3+} center with the nearest-neighbors.¹² We do not discuss in this work the reason why the triplet form of the absorption band arises in the fields at small angles with the trigonal axis. Nevertheless, the characteristic width of the non-uniformly widened ESR line and splitting between the elements of its fine structure can serve as an estimate of spin-spin interaction energy that is used further in the model calculations.

The heat capacity study on monocrystalline $\text{ErAl}_3(\text{BO}_3)_4$ was conducted by using the relaxation method with equipment Physical Property Measurement System (PPMS), Quantum Design company. The measurement uncertainty of the heat capacity changed from $1 \cdot 10^{-4}$ to $8 \cdot 10^{-4}$ J/(mol·K) at temperatures ranging from 2 to 7 K and did not exceed $1,3 \cdot 10^{-3}$ J/(mol·K) at temperatures below 9,5 K. The measurements were performed without an external magnetic field. The temperature dependence

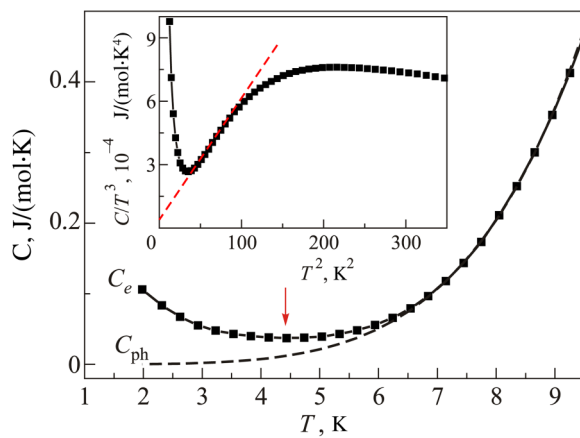


FIG. 2. Temperature dependence of heat capacity C_e of crystalline $\text{ErAl}_3(\text{BO}_3)_4$, measured without external magnetic field (solid line). The arrow defines the minimum of dependence. The dashed line shows the phonon contribution to heat capacity C_{ph} , as deduced from the formula (1). The calculated coefficients b and a were determined from the slope of dashed line and cutoff with y -coordinate from the dependence $C_e/T^3(T^2)$ shown in the inset.

of heat capacity C_e in Fig. 2 displays minimum at $T \approx 4,5$ K. Increasing the sample temperature from 2 K initially leads to lower heat capacity, and only at $T \geq 4,5$ K, the value C_e begins to grow with increasing intensity. Such a behavior in the dependence of $C_e(T)$ points to the existence of magnetic contribution to the heat capacity of the sample at low temperatures.

From results of spectroscopic studies on $\text{ErAl}_3(\text{BO}_3)_4$,⁷ the main doublet of the rare-earth ion multiplet $^4I_{15/2}$ split by crystal field is separated from the first excited doublet by a rather large value ~ 46 cm^{-1} . Consequently, considering a range of low enough temperatures, we neglected a Schottky anomaly related contribution to heat capacity. Therefore, the magnetic part of heat capacity C_m can be determined by subtracting the phonon part of heat capacity C_{ph} from the experimental data.

To describe C_{ph} , one can use the expression from:¹³

$$C_{\text{ph}} = aT^3 + bT^5. \quad (1)$$

The calculated coefficients $b = 5,8 \cdot 10^{-6}$ J/(mol·K⁶) and $a = 2,4 \cdot 10^{-5}$ J/(mol·K⁴) were determined from the dependence $C_e/T^3(T^2)$ using the slope of the dashed line and its cutoff with the y -axis, respectively, as shown in the insert to Fig. 2. The result of the calculated value C_{ph} is mainly displayed in Fig. 2 with the dashed line. The value C_{ph} almost ideally matches the value C_e at $T \geq 7$ K. At lower temperatures, one obtains positive $C_m = C_e - C_{\text{ph}}$, for which Fig. 3 displays the temperature dependence in linear (a) and logarithmic scales (b). From the slope of the line in Fig. 3(b), one can infer that the dependence $C_m(T)$ in the temperature range from 1,9 to 4,5 K is close to inverse proportionality to T^2 . Such a dependence is characteristic to crystals comprising interacting magnetic ions at temperatures far exceeding the temperature of ordering.

3. DISCUSSION

To estimate the correspondence of the obtained dependence $C_m(T)$ to the ESR data, let us consider the simplest case when the magnetic subsystem of a crystal is represented as an ensemble of clusters, each of which consists of a pair of rare-earth ions. At low temperatures, one can take into account only the lowest doublet since other levels of a rare-earth ion are separated from it with a large energy gap and, therefore, sparsely populated. Let us write the Hamiltonian \mathcal{H}_0 of a pair of effective spins 1/2 (for brevity, hereafter defined as spins) in the external magnetic field directed along the z -axis

$$\mathcal{H}_0 = J_x S_1^x S_2^x + J_y S_1^y S_2^y + J_z S_1^z S_2^z - g_z \mu_B H_z (S_1^z + S_2^z), \quad (2)$$

where $S_{1,2}^{x,y,z}$ are operators of the projections of spins 1 or 2, respectively, and $J_{x,y,z}$ are the values of constants of spin-spin interaction, normalized to the Boltzmann constant k , μ_B is the Bohr magneton, g_z is the value of the effective g -factor for the pairs, and H_z is the magnitude of projection of the external magnetic field. At $J_x = J_y = J_z$ anisotropy is not present. In the given representation, a positive J corresponds to the antiferromagnetic type of interaction and negative — to ferromagnetic.

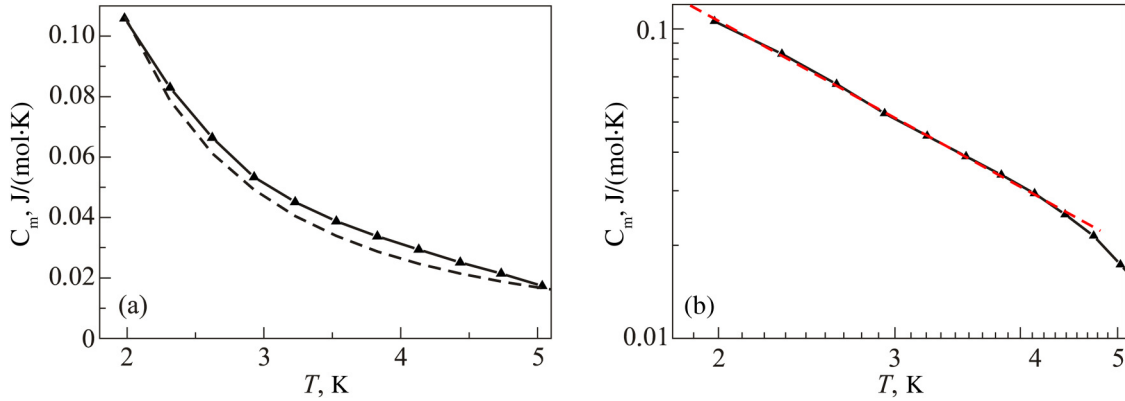


FIG. 3. Temperature dependence of magnetic contribution C_m to the heat capacity of $\text{ErAl}_3(\text{BO}_3)_4$ crystal depicted in linear (a) and logarithmic (b) coordinates. The solid lines correspond to the difference $C_e - C_{\text{ph}}$. The results of calculations according to the formula (3) are shown in (a) with the dashed line. The value of inclination angle depicted with the dashed line in (b) determines the power exponent of proportionality $C_m(T) \sim 1/T^{1.78}$.

Eigenvalues of Hamiltonian \mathcal{H}_0 at $\mathbf{H} \parallel z$ are equal to

$$E_{1,2} = -(J_z/4) \pm (J_x + J_y)/4,$$

$$E_{3,4} = (J_z/4) \pm [(g_z \mu_B H_z)^2 + (J_x - J_y)^2/16]^{1/2}.$$

Energy E_2 in the case of isotropic interaction corresponds to a singlet state of a pair with the total spin $S = 0$, and energy $E_{1,3,4}$ corresponds to the triplet state of a pair with the total spin $S = 1$ and the projections of total spin equal to 0, 1, and -1 , respectively. ESR gives rise to transitions with frequencies

$$h\nu_1 = \left| [(g_z \mu_B H_z)^2 + (J_x - J_y)^2/16]^{1/2} + (J_z/2) - (J_x + J_y)/4 \right|$$

and

$$h\nu_2 = \left| [(g_z \mu_B H_z)^2 + (J_x - J_y)^2/16]^{1/2} + (J_z/2) - (J_x + J_y)/4 \right|.$$

This corresponds to the values of initial splitting $\Delta_z = |(J_z - J_y)/2|$ and $|(J_z - J_x)/2|$. The expression for field-frequency dependence of the ESR spectrum along x and y directions can be determined by cyclic substitution of indexes (z, x, y) to (y, z, x) and (x, y, z) .

Let us calculate the magnetic component of one-molar heat capacity of ions when paired clusters take the full sample volume. Defining the universal gas constant as R , in zero field one obtains

$$C_m = \frac{R}{(4T)^2 \left[\text{ch} \left(\frac{J_x + J_y}{4T} \right) + \exp \left(-\frac{J_z}{2T} \right) \text{ch} \left(\frac{J_x - J_y}{4T} \right) \right]^2} \left([J_x + J_y]^2 - \exp \left(-\frac{J_z}{T} \right) [J_x - J_y]^2 + 2 \exp \left(-\frac{J_z}{2T} \right) \right. \\ \times \left[(J_x^2 + J_y^2 + 2J_z^2) \text{ch} \left(\frac{J_x + J_y}{4T} \right) \text{ch} \left(\frac{J_x - J_y}{4T} \right) - (J_x^2 - J_y^2) \text{sh} \left(\frac{J_x + J_y}{4T} \right) \text{sh} \left(\frac{J_x - J_y}{4T} \right) \right. \\ \left. \left. + 2J_z(J_x + J_y) \text{sh} \left(\frac{J_x + J_y}{4T} \right) \text{ch} \left(\frac{J_x - J_y}{4T} \right) - 2J_z(J_x - J_y) \text{sh} \left(\frac{J_x - J_y}{4T} \right) \text{ch} \left(\frac{J_x + J_y}{4T} \right) \right] \right). \quad (3)$$

Figure 3(a) presents the calculation results for $C_m(T)$ according to the formula (3) at $J_z/k = 0,1$ K, $J_x/k = -0,86$ K and $J_y/k = -0,23$ K. The calculation agrees well with $C_m = C_e - C_{\text{ph}}$. By supposing that z is directed along the trigonal direction of crystal c , and x — along the second-order axis a , one obtains $\Delta_z = |(J_z - J_y)/2| = 0,165$ K and $\Delta_x = |(J_x - J_z)/2| = 0,48$ K. These values of initial splitting correspond to the values $\Delta_{2c}/2$ and $\Delta_{2a}/2$ obtained from the ESR measurements. Using the formula (3) for calculation and comparing with $C_e - C_{\text{ph}}$

one must consider two factors. Firstly, the clusters can occupy the partial sample volume. In this case, one must calculate the concentration of clusters that will result in a lower calculated C_m value at fixed J_{xyz} values. Secondly, the clusters can comprise more than two spins. Therefore, the mentioned J_{xyz} values are considered as a rough estimate of the constants of spin-spin interaction. Further studies on the behavior of heat capacity in an external magnetic field as well as at lower temperatures can

provide more detailed information about spin-spin interaction in erbium aluminum borate.

Er^{+3} ion in the studied monocrystal bears a rather large magnetic moment. Therefore, one should consider dipolar interaction as contributing to the formation of magnetic clusters in $\text{ErAl}_3(\text{BO}_3)_4$. Estimated value of energy of this interaction, for instance, along the second-order axis a , $(g_{1a\mu_B})^2/kr^3 \approx 0,24$ K (the shortest distance between Er^{+3} ions r is $5,866 \text{ \AA}$).¹⁴ Since the order of magnitude is the same as J , one can suppose that magneto-dipole interaction between erbium ions makes a substantial contribution to the formation of short-range magnetic order.

4. CONCLUSIONS

At 4,2 K, we observed resonance due to magneto-coupled groups of rare-earth ions in monocrystal $\text{ErAl}_3(\text{BO}_3)_4$. At temperatures of liquid helium, magnetic contribution to heat capacity is revealed. The results of calorimetry and ESR-spectroscopy suggest manifestation of short-order in erbium aluminum borate.

The authors express gratitude to A. I. Krivchikov for aiding with discussion of research results.

REFERENCES

- ¹P. Dekker, J. M. Dawes, J. A. Piper, Y. G. Liu, and J. Y. Wang, *Opt. Commun.* **195**, 431 (2001).
- ²F. Yang, Y. Liang, M. Liu, X. Li, X. Wu, and N. Wang, *Optik (Optics)* **124**, 2004 (2013).

- ³K.-C. Liang, R. P. Chaudhury, B. Lorenz, Y. Y. Sun, L. N. Bezmaternykh, V. L. Temerov, and C. W. Chu, *Phys. Rev. B* **83**, 180417 (2011).
- ⁴M. I. Pashchenko, V. A. Bedarev, D. N. Merenkov, A. N. Bludov, V. A. Pashchenko, S. L. Gnatchenko, T. Zajarniuk, A. Szewczyk, and V. L. Temerov, *Low Temp. Phys.* **43**, 631 (2017).
- ⁵K.-C. Liang, R. P. Chaudhury, B. Lorenz, Y. Y. Sun, L. N. Bezmaternykh, I. A. Gudim, V. L. Temerov, and C. W. Chu, *J. Phys. Conf. Series* **400**, 032046 (2012).
- ⁶A. V. Malakhovskii, T. V. Kutsak, A. L. Sukhachev, A. S. Aleksandrovsky, A. S. Krylov, I. A. Gudim, and M. S. Molokeev, *Chem. Phys.* **428**, 137 (2014).
- ⁷A. V. Malakhovskii, V. V. Sokolov, and I. A. Gudim, *J. Alloys and Comp.* **698**, 364 (2017).
- ⁸V. A. Bedarev, D. N. Merenkov, M. I. Kobets, S. N. Poperezhaj, S. L. Gnatchenko, and I. A. Gudim, *Low Temp. Phys.* **44**, 863 (2018).
- ⁹V. A. Bedarev, M. I. Paschenko, M. I. Kobets, K. G. Dergachev, E. N. Khatsko, S. L. Gnatchenko, A. A. Zvyagin, T. Zajarniuk, A. Szewczyk, M. U. Gutowska, L. N. Bezmaternykh, and V. L. Temerov, *Low Temp. Phys.* **41**, 534 (2015).
- ¹⁰M. Date and M. Motokawa, *Phys. Rev. Lett.* **16**, 1111 (1966); *J. Phys. Soc. Jpn.* **24**, 41 (1968).
- ¹¹M. I. Kobets, E. N. Khatsko, V. A. Pashchenko, A. S. Chernyi, K. G. Dergachev, and V. G. Borisenko, *Low Temp. Phys.* **28**, 889 (2002).
- ¹²A. Abragam and B. Bleaney, *Electron Paramagnetic Resonance of Transition Ions* (Clarendon Press, Oxford, 1970).
- ¹³A. Tari, *Specific Heat of Matter at Low Temperatures* (Imperial College Press, London 2003).
- ¹⁴E. Sváb, E. Beregi, M. Fábrián, and Gy. Mészáros, *Optical Materials* **34**, 1473 (2012).

Translated by AIP Author Services